Check for updates

VIP Metal–Organic Frameworks Very Important Paper

International Edition: DOI: 10.1002/anie.201813494
German Edition: DOI: 10.1002/ange.201813494

Metal–Organic-Framework-Derived Hollow N-Doped Porous Carbon with Ultrahigh Concentrations of Single Zn Atoms for Efficient Carbon Dioxide Conversion

*Qihao Yang, Chun-Chuen Yang, Chia-Her Lin, and Hai-Long Jiang**

Dedicated to Professor Jin-Shun Huang on the occasion of his 80th birthday

Abstract: *The development of efficient and low energy-consumption catalysts for CO_2 conversion is desired, yet remains a great challenge. Herein, a class of novel hollow porous carbons (HPC), featuring well dispersed dopants of nitrogen and single Zn atoms, have been fabricated, based on the templated growth of a hollow metal–organic framework precursor, followed by pyrolysis. The optimized HPC-800 achieves efficient catalytic CO_2 cycloaddition with epoxides, under light irradiation, at ambient temperature, by taking advantage of an ultrahigh loading of (11.3 wt %) single-atom Zn and uniform N active sites, high-efficiency photothermal conversion as well as the hierarchical pores in the carbon shell. As far as we know, this is the first report on the integration of the photothermal effect of carbon-based materials with single metal atoms for catalytic CO_2 fixation.*

Ocean acidification and global warming, caused by greenhouse gases (mainly CO_2), have attracted extensive attention. Different strategies and materials, such as amine-based wet scrubbing and solid porous adsorbents, etc., for CO_2 capture and sequestration from industrial streams have been developed.[1] Meanwhile, as a plentiful C1 resource, CO_2 can be converted into various value-added products.[2,3] There is an increasing interest in utilizing CO_2 as a resource of crude materials, rather than a trash with processing costs.

From the perspective of green and sustainable chemistry, the synthesis of cyclic carbonates via coupling of epoxides and CO_2 is very promising, not only because of the high atom economy, but also due to the valuable products widely used in industry.[3] To date, while various types of homogeneous catalysts, including Schiff bases, ionic liquids, metal complexes, etc., were reported for this reaction,[3e–h] they suffer from intrinsic difficulty in product separation and catalyst recycling. Therefore, it is highly desired to seek heterogeneous catalysts with very active sites. The conventional solid heterogeneous catalysts, such as zeolites, metal–organic frameworks (MOFs), mesoporous oxides, porous polymers, etc., usually require moderately high temperatures to drive this reaction, due to the inert nature of CO_2.[3a,4] In view of energy and cost, the development of efficient heterogeneous catalysts for the reaction at ambient temperature is extremely desirable. To this end, it would be ideal to utilize solar energy, instead of heating, to drive the endothermic reaction via the photothermal effect of catalysts. As an important class of photothermal agents, carbon-based materials have been intensively studied.[5] Owing to their wide spectral absorption, solar light can be effectively harvested and then released into the surrounding environment via thermal radiation. Moreover, it is generally accepted that the hollow structure allows the multiple reflection of light within the inner voids,[6] which is beneficial to photothermal effect and thus improves the activity for the endothermic CO_2 cycloaddition with epoxides. The main challenge for pure carbon materials lies in the lack of active sites and the weak interaction with CO_2 molecules, making them relatively inert for CO_2 cycloaddition reactions. To address this issue, incorporating Lewis acid sites (such as single-atom metal sites) and Lewis base sites (such as pyridinic N) into porous carbons, thereby synergistically activating the epoxides and CO_2 molecules, might be a judicious solution.

Bearing the above considerations in mind, we have rationally fabricated the hollow porous carbon (HPC) featuring uniform N doping and ultrahigh loading (11.3 wt %) of single Zn atoms, via the pyrolysis of a hollow structured, Zn-based N-rich MOF, termed ZIF-8 (Scheme 1).[7] The obtained HPC possesses the following advantages: 1) the porous shell with high surface area can enrich CO_2 molecules and enhance the catalytic activity; 2) the porous shell facilitates the transport of substrates/products; 3) the atomically dispersed Zn/N active sites are readily available for epoxide and CO_2; 4) the hollow structure improves solar energy harnessing via multiple reflection of light. As a result, the HPC exhibits excellent catalysis in the CO_2 cycloaddition with epoxides, under light irradiation at ambient temperature. Notably, although MOF-derived porous carbons have been widely studied for catalysis in recent years,[8] this work is the first report on the integration

[*] Q. Yang, Prof. H.-L. Jiang
Hefei National Laboratory for Physical Sciences at the Microscale, CAS Key Laboratory of Soft Matter Chemistry, Collaborative Innovation Center of Suzhou Nano Science and Technology, Department of Chemistry, University of Science and Technology of China
Hefei, Anhui 230026 (P. R. China)
E-mail: jianglab@ustc.edu.cn
Homepage: http://staff.ustc.edu.cn/~jianglab/
Prof. C.-C. Yang, Prof. C.-H. Lin
Department of Chemistry, Chung Yuan Christian University
Taoyuan 32023 (Taiwan)
Supporting information and the ORCID identification number(s) for the author(s) of this article can be found under: https://doi.org/10.1002/anie.201813494.

 © 2019 Wiley-VCH Verlag GmbH & Co. KGaA, Weinheim

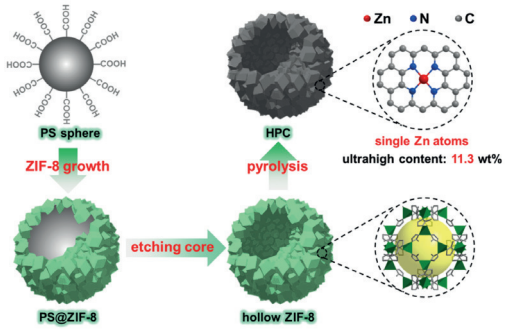

Scheme 1. Schematic illustration showing the fabrication process of the HPC.

of the photothermal effect of carbon-based materials with single metal atoms for catalytic CO_2 fixation.

The polystyrene (PS) nanospheres modified with carboxylic acids on their external surface were synthesized according to the previous report.[9] Subsequently, ZIF-8 nanoparticles were assembled on the surface of the PS nanosphere to give the PS@ZIF-8 core–shell composite (Scheme 1). Following that, the PS core was removed by soaking the composite in N,N-dimethyl formamide to give hollow ZIF-8 (denoted as H-ZIF-8). Powder X-ray diffraction (XRD) patterns of PS@ZIF-8 and H-ZIF-8 indicate that ZIF-8 is obtained and its crystallinity is well retained upon PS removal (Supporting Information, Figure S1). Scanning electron microscopy (SEM) images show that the average size of the PS core is approximately 210 nm, while that of PS@ZIF-8 is approximately 260 nm, indicating that the average thickness of the ZIF-8 shell is approximately 25 nm, which is further confirmed by transmission electron microscopy (TEM) image of H-ZIF-8 (Supporting Information, Figure S2). The H-ZIF-8 spheres were pyrolyzed at different temperatures under N_2 atmosphere to give HPC (denoted as HPC-T, $T = 600$, 700, 800, 900, and 1000 °C, Scheme 1).

The SEM image shows that the shell in all HPC-T samples is assembled by the interconnected pyrolyzed ZIF-8 nanoparticles (Figure 1a and Supporting Information, Figure S3).

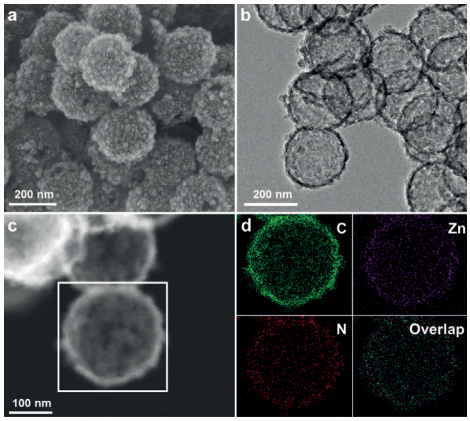

Figure 1. The a) SEM, b) TEM, and c) HAADF-STEM images of HPC-800. d) The corresponding elemental mapping of C (green), Zn (purple), and N (red) for the selected area in (c).

As a representative, both TEM and high-angle annular dark-field scanning TEM (HAADF-STEM) observations indicate that HPC-800 features the hollow structure, similar to the original H-ZIF-8 (Figure 1b and 1c, and Supporting Information, Figure S2d), however it has decreased to approximately 230 nm in size. Elemental mapping indicates that the HPC-800 is mainly composed of C, N, and Zn. N and Zn are evenly distributed throughout the carbon shell (Figure 1d), highlighting the niche of the MOF precursor.

The diffraction peak of Zn or ZnO species cannot be observed in the powder XRD profiles of all of HPC-T samples (Supporting Information, Figure S4a), implying the possibly low content or/and small sizes of the Zn species in the pyrolysis products. The broad peak at approximately 25 degrees can be assigned to the (002) diffraction of graphitic carbon,[10] as further confirmed by the Raman scattering spectrum (Supporting Information, Figure S4b). To our surprise, while no Zn particles can be found in the high-resolution TEM (HRTEM) image (Supporting Information, Figure S4c), the Zn content is as high as 11.3 wt% in HPC-800, as determined by inductively coupled plasma (ICP) analysis. To determine the form of the Zn species, aberration-corrected HAADF-STEM observation was conducted, which unambiguously shows that all Zn are atomically dispersed on the carbon matrix (Figures 2a). A close examination of different regions reveals that no Zn nanoparticles can be found in HPC-800 (Supporting Information, Figure S5). It should be noted that a high content of metal active sites in single-atom catalysts is a long-term goal and such a metal loading (11.3 wt%) is among the highest in all reported single-atom catalysts (Supporting Information, Table S1).[11] To our knowledge, this is the highest content of single-atom Zn in a catalyst reported thus far.[11a]

X-ray photoelectron spectroscopy (XPS) measurements for HPC-800 suggest the presence of C, N, Zn, and O elements (Supporting Information, Figure S6). The N 1s spectrum exhibits three peaks with binding energies of 398.5, 399.7, and

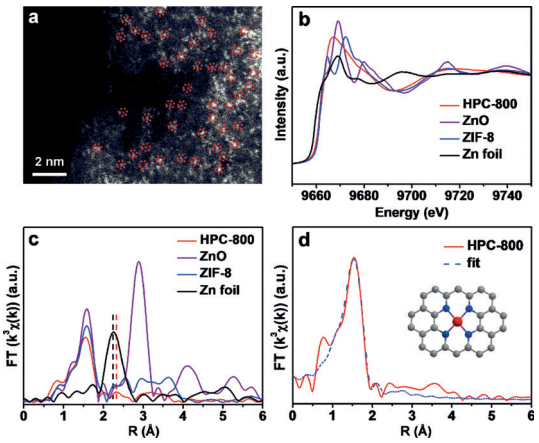

Figure 2. a) The aberration-corrected HAADF-STEM image of HPC-800 (single-atom Zn is highlighted with red circles). b) Zn K-edge XANES and c) k^3-weighted Fourier transform of EXAFS spectra. The dashed lines highlight the peak difference between Zn foil and HPC-800. d) The EXAFS R-space fitting curve of HPC-800 (Inset: model of HPC-800, Zn is shown in red, N is shown in blue, and C is shown in gray).

 © 2019 Wiley-VCH Verlag GmbH & Co. KGaA, Weinheim

401 eV, corresponding to pyridinic N, pyrrolic N, and graphitic N,[12] respectively, which might serve as coordination sites for Zn atoms. The lower binding energy of $2p_{3/2}$ of Zn species than ZnO[11a] infers that ZnO is not the predominant species in HPC-800.

To elucidate the form of the zinc species in HPC-800, X-ray absorption spectroscopy (XAS), a powerful technique to determine the coordination environment and valence state of the target atoms was adopted. As shown in X-ray absorption near-edge structure (XANES) spectra (Figure 2b), the position of the absorption threshold for HPC-800 is located between those of Zn foil and ZIF-8, but closer to ZIF-8, indicating that the valence state of the Zn species in HPC-800 is probably situated between 0 and +2 (close to +2). This result is further verified by the differential curve comparison based on the XANES data (Supporting Information, Figure S7). Moreover, the extended X-ray absorption fine structure (EXAFS) spectra further reveal that HPC-800 and ZIF-8 exhibit similar Zn–N coordination with a peak at about 1.6 Å (Figure 2c). However, the slightly lower R-position in the Zn–N peak for HPC-800 indicates that the Zn atom in the pyrolysis product is slightly different from the tetrahedral coordination in the parent ZIF-8. Importantly, the fingerprinting signal peaks of Zn–Zn interactions in Zn foil (2.3 Å) and ZnO (2.9 Å) are not observed in the profile of HPC-800, manifesting the atomic dispersion of Zn in HPC-800. The best fitting result of the obtained EXAFS data reveals that $Zn–N_4$ is the dominant coordination mode of Zn atoms in HPC-800 (Figure 2d and Supporting Information, Figure S8 and Table S2). These results indicate that the abundant N atoms in H-ZIF-8 are crucial in stabilizing the high content of single-atom Zn and avoiding the formation of Zn particles.

The porous character of all HPC-T samples has been investigated by N_2 sorption (Supporting Information, Table S3). The sorption curves and the pore size distribution analysis suggest the presence of hierarchical pores in all samples (Supporting Information, Figures S9 and S10). Apart from micropores, a considerable amount of pores fall into the mesopore and macropore ranges. The micropore is beneficial to the CO_2 enrichment, whereas mesopores and macropores would facilitate the transport of substrates/products. To examine the CO_2 capture capability of HPC-800, the CO_2 sorption has been measured to give 98.6 and 67.7 $cm^3 g^{-1}$ at 1 bar at 273 and 298 K, respectively, (Supporting Information, Figure S11), which represents a moderately high level and is comparable to those of other porous materials.[4c,13]

Remarkably, HPC-800 exhibits a broad photoresponse in the range of 230–800 nm, which almost covers ultraviolet and visible regions of sunlight (Supporting Information, Figure S12). The photothermally driven cycloaddition of CO_2 with 3-bromopropylene oxide under light irradiation was first chosen to explore the optimized reaction parameters (Table 1). Among all pyrolysis products, HPC-800 presents the highest catalytic yield (94%) under identical conditions (entries 1–5 in Table 1). To evaluate the photothermal effect of HPC-800, the temperature of the solution was detected during the reaction. Results show that light can be efficiently converted into heat with HPC-800 (Supporting Information, Figure S13). Since temperature is critical to the CO_2 cycloaddition reaction, the yield is sharply reduced to <5% without light irradiation (entry 6 in Table 1), manifesting the vital importance of photothermal effect for this reaction. Moreover, the catalytic activity of HPC-800 is greatly affected by the light intensity (Supporting Information, Figure S14). Furthermore, in the absence of HPC-800, tetrabutyl ammonium bromide (TBAB), or CO_2, the target product is greatly reduced or even undetectable (entries 7–9 in Table 1). Obviously, all of these components are essential for the catalytic CO_2 cycloaddition. Moreover, the type of co-catalyst plays a crucial role in this reaction. When TBAB is replaced by tetrabutyl ammonium chloride (TBAC), the conversion reduces to 60% (entry 10 in Table 1). The larger ionic radius of Br^- in comparison to Cl^- results in the easier separation of Br^- from TBA^+.[14a] Moreover, the stronger nucleophilic effect of Br^- than that of Cl^- makes Br^- more effective at attacking epoxide.[14b] These two factors finally lead to the better catalytic activity of TBAB. Furthermore, the wavelength range of the light source is another crucial factor. When the light source is cut to visible light (400–800 nm), the yield of the target product sharply reduces to 51% (entry 11 in Table 1).

To demonstrate the advantages of the unique hollow structure of HPC-800 for catalysis, a control experiment with the product of pyrolyzing ZIF-8 particles at 800 °C (denoted ZIF-8-800) was conducted. Only 58% conversion was achieved when using ZIF-8-800 under similar conditions (entry 12 in Table 1). For further direct comparison, the hollow structure of HPC-800 was deliberately destroyed

Table 1: Catalytic cycloaddition reaction of 3-bromopropylene oxide and CO_2 under different conditions.[a]

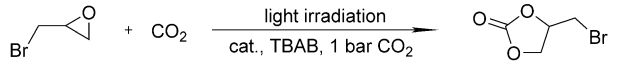

Entry	Catalyst	CO_2 [bar]	Co-catalyst	Yield [%][b]
1	HPC-600	1	TBAB	77
2	HPC-700	1	TBAB	87
3	HPC-800	1	TBAB	94
4	HPC-900	1	TBAB	62
5	HPC-1000	1	TBAB	39
6[c]	HPC-800	1	TBAB	<5
7[d]	–	1	TBAB	<5
8[e]	HPC-800	1	–	14
9[f]	HPC-800	–	TBAB	–
10[g]	HPC-800	1	TBAC	60
11[h]	HPC-800	1	TBAB	51
12	ZIF-8-800	1	TBAB	58
13	HPC-800-smashed	1	TBAB	65
14	HPC-800-P	1	TBAB	70
15	HPC-800-C	1	TBAB	52
16	AC	1	TBAB	<5
17[i]	HPC-800	0.15	TBAB	90

[a] Reaction conditions: 0.15 mmol 3-bromopropylene oxide, 30 mg catalyst, 0.1 mmol TBAB, 3 mL DMF, 1 bar CO_2, 300 mW cm^{-2} full-spectrum irradiation, 10 h. [b] Products were analyzed and identified by gas chromatography. [c] No light irradiation. [d] No catalyst. [e] No TBAB. [f] 1 bar CO_2 was replaced with 1 bar N_2. [g] Co-catalyst was replaced with 0.1 mmol TBAC. [h] Full-spectrum irradiation was replaced with visible irradiation. [i] 1 bar CO_2 was replaced with a mixture gas (0.15 bar CO_2, 0.85 bar N_2), and the reaction was extended to 30 h.

 © 2019 Wiley-VCH Verlag GmbH & Co. KGaA, Weinheim

(denoted as HPC-800-smashed) using an ultrasonic disintegrator (Supporting Information, Figure S15). As expected, without the unique hollow structure, the yield of target product drops to 65% (entry 13 in Table 1). All of these results explicitly indicate that the unique hollow structure plays a critical role in light harvesting to enhance the activity of the CO_2 cycloaddition. To evaluate the significance of single-atom Zn for the catalysis, single Zn atoms in HPC-800 were partially or (almost) completely removed to give HPC-800-P (2.87 wt% Zn content) and HPC-800-C (0.08 wt% Zn content) for control studies. Significantly, the yield of the target product sharply drops to 70% and 52% when using HPC-800-P and HPC-800-C, respectively, with other reaction parameters fixed (entries 14 and 15 in Table 1 and Supporting Information, Table S4). Moreover, a ZnO/AC (AC: activated carbon) catalyst was prepared for comparison. The yield of target product is greatly reduced to 54% when using ZnO/AC under similar conditions (Supporting Information, Figure S16). All of these results verify the critical role of single Zn atoms. To demonstrate the role of the N species, using N-free activated carbon as a catalyst gives no product under similar conditions (entry 16 in Table 1), which is significantly different from the yield (52%) obtained when using N-doped catalyst (HPC-800-C). The result obviously illustrates that the uniformly doped N atoms are helpful to this reaction. The single Zn atoms in the $Zn^{\delta+}$ $(0<\delta<2)$ oxidation state, possessing empty orbitals to accept electrons, would serve as Lewis acid sites, together with the Lewis base sites from their surrounding N atoms, synergistically promote the reaction. The CO_2 capture capability and the photothermal effect of HPC-800 further boost the cycloaddition reaction to give the excellent efficiency. On the basis of preceding results, a tentative reaction mechanism of HPC-800 has been proposed (Scheme S1).

To verify the nature of the heterogeneous catalysis of HPC-800, the filtration test was carried out after 4 h of reaction. No further product can be detected, even after 6 h of reaction, upon the removal of the catalyst while other conditions remain, which reflects that the process should be truly heterogeneous (Supporting Information, Figure S17). More importantly, the activity and unique hollow structure of the catalyst can be well maintained during the three runs, indicating the recyclability and the stability of HPC-800 (Supporting Information, Figure S18). The powder XRD pattern for HPC-800 after the reaction is similar to that before reaction and does not show an identifiable diffraction peak of Zn or ZnO species (Supporting Information, Figure S19). The EXAFS spectrum and aberration-corrected HADDF-STEM observation for HPC-800 after three catalytic cycles reveals that the Zn species are almost retained in the single atom form (Supporting Information, Figure S20). In order to investigate the catalyst performance under practical conditions, a mixture of gas containing 0.15 bar CO_2 and 0.85 bar N_2, simulating flue gas from a power plant, was employed for the cycloaddition reaction.[13c,d] Delightedly, the yield can reach up to 90% with extended reaction time (entry 17 in Table 1), indicating that HPC-800 is an excellent heterogeneous catalyst for the CO_2 capture and subsequent conversion with epoxides.

Encouraged by the above superior performance of HPC-800 for the CO_2 cycloaddition with 3-bromopropylene oxide, various epoxides with different functional groups were further investigated (Supporting Information, Table S5). To our delight, good to excellent conversions can be achieved in almost all reactions, indicating the great substrate tolerance of the catalyst. All small epoxides with electron-withdrawing/-donating groups can be efficiently converted (entries 1–3 in Table S5). In comparison, considering the steric hindrance effect of large substituents, both 2-(phenoxymethyl)-oxirane and 1,2-epoxyhexane give relatively low reaction rates (entries 4 and 5 in Table S5). Of these two substrates, the activity of 2-(phenoxymethyl)-oxirane is higher, in which the electron-withdrawing group (-OPh) makes the substrate more susceptible to Br^- attack from TBAB, accelerating the reaction. As an exception, the catalyst gives relatively low yield (67%) for styrene oxide conversion, even when the reaction time is extended to 48 h (entry 6 in Table S5), which might be due to the strong interaction between the epoxy group and benzene ring.

In summary, we have rationally fabricated a series of HPC catalysts with uniform N doping and ultrahigh loading of single Zn atoms in the carbon shell, based on the pyrolysis of hollow MOF spheres, for catalytic CO_2 cycloaddition with epoxides. The hollow-structured porous carbon, which allows multiple reflections of light within the interior cavity, can efficiently harvest solar energy in a broad UV–visible range and convert it into heat, significantly boosting the endothermic CO_2 conversion. Meanwhile, the ultrahigh content of single Zn atoms is stabilized by the surrounding N atoms to give $Zn–N_4$ units, in which Zn and N behave as a Lewis acid site and a Lewis base site, respectively, and cooperate to promote the substrate activation. Furthermore, the hierarchically porous character of the carbon shell facilitates CO_2 enrichment and rapid transport of substrates/products. As a result, the optimal HPC-800 is capable of efficiently catalyzing the CO_2 cycloaddition reaction under light irradiation at ambient temperature. Moreover, the structure and activity of the catalyst are well retained during recycling experiments. This work represents not only the first attempt on introducing single atoms but also the first integration of the photothermal effect into the endothermic CO_2 cycloaddition. This combination synergistically promotes the catalytic process. We envision that the current strategy, based on MOF precursors, for the formation of single-atom catalysts featuring significant photothermal effect will open an avenue for the enhanced catalysis toward diverse reactions.

Acknowledgements

This work is supported by the NSFC (21725101, 21871244, 21673213, 21521001), the 973 program (2014CB931803), Fundamental Research Funds for the Central Universities (WK2060030029), BSRF, SSRF and Fujian Institute of Innovation (CAS).

 © 2019 Wiley-VCH Verlag GmbH & Co. KGaA, Weinheim

Conflict of interest

The authors declare no conflict of interest.

Keywords: carbon materials · CO_2 cycloaddition · metal–organic frameworks · photothermal effect · single-atom catalysis

How to cite: *Angew. Chem. Int. Ed.* **2019**, *58*, 3511 –3515
Angew. Chem. **2019**, *131*, 3549 –3553

[1] a) S. Choi, J. H. Drese, C. W. Jones, *ChemSusChem* **2009**, *2*, 796; b) N. MacDowell, N. Florin, A. Buchard, J. Hallett, A. Galindo, G. Jackson, C. S. Adjiman, C. K. Williams, N. Shah, P. Fennell, *Energy Environ. Sci.* **2010**, *3*, 1645.

[2] a) W. Wang, S. Wang, X. Ma, J. Gong, *Chem. Soc. Rev.* **2011**, *40*, 3703; b) I. Omae, *Coord. Chem. Rev.* **2012**, *256*, 1384; c) J. Qiao, Y. Liu, F. Hong, J. Zhang, *Chem. Soc. Rev.* **2014**, *43*, 631; d) H.-Q. Xu, J. Hu, D. Wang, Z. Li, Q. Zhang, Y. Luo, S.-H. Yu, H.-L. Jiang, *J. Am. Chem. Soc.* **2015**, *137*, 13440; e) C. A. Trickett, A. Helal, B. A. Al-Maythalony, Z. H. Yamani, K. E. Cordova, O. M. Yaghi, *Nat. Rev. Mater.* **2017**, *2*, 17045.

[3] a) H. He, J. A. Perman, G. Zhu, S. Ma, *Small* **2016**, *12*, 6309; b) Y. Zhang, J. Y. G. Chan, *Energy Environ. Sci.* **2010**, *3*, 408; c) X.-B. Lu, D. J. Darensbourg, *Chem. Soc. Rev.* **2012**, *41*, 1462; d) R. R. Shaikh, S. Pornpraprom, V. D'Elia, *ACS Catal.* **2018**, *8*, 419; e) A. Decortes, A. M. Castilla, A. W. Kleij, *Angew. Chem. Int. Ed.* **2010**, *49*, 9822; *Angew. Chem.* **2010**, *122*, 10016; f) M. North, R. Pasquale, C. Young, *Green Chem.* **2010**, *12*, 1514; g) B.-H. Xu, J.-Q. Wang, J. Sun, Y. Huang, J.-P. Zhang, X.-P. Zhang, S.-J. Zhang, *Green Chem.* **2015**, *17*, 108; h) C. Maeda, T. Taniguchi, K. Ogawa, T. Ema, *Angew. Chem. Int. Ed.* **2015**, *54*, 134; *Angew. Chem.* **2015**, *127*, 136.

[4] a) C. M. Miralda, E. E. Macias, M. Zhu, P. Ratnasamy, M. A. Carreon, *ACS Catal.* **2012**, *2*, 180; b) M. H. Beyzavi, R. C. Klet, S. Tussupbayev, J. Borycz, N. A. Vermeulen, C. J. Cramer, J. F. Stoddart, J. T. Hupp, O. K. Farha, *J. Am. Chem. Soc.* **2014**, *136*, 15861; c) G. Ji, Z. Yang, H. Zhang, Y. Zhao, B. Yu, Z. Ma, Z. Liu, *Angew. Chem. Int. Ed.* **2016**, *55*, 9685; *Angew. Chem.* **2016**, *128*, 9837; d) D. Liu, G. Li, J. Liu, Y. Wei, H. Guo, *ACS Appl. Mater. Interfaces* **2018**, *10*, 22119; e) D. Feng, W.-C. Chung, Z. Wei, Z.-Y. Gu, H.-L. Jiang, Y.-P. Chen, D. J. Darensbourg, H.-C. Zhou, *J. Am. Chem. Soc.* **2013**, *135*, 17105.

[5] a) H. K. Moon, S. H. Lee, H. C. Choi, *ACS Nano* **2009**, *3*, 3707; b) S. Wang, L. Shang, L. Li, Y. Yu, C. Chi, K. Wang, J. Zhang, R. Shi, H. Shen, G. I. N. Waterhouse, S. Liu, J. Tian, T. Zhang, H. Liu, *Adv. Mater.* **2016**, *28*, 8379.

[6] a) H. Li, Z. Bian, J. Zhu, D. Zhang, G. Li, Y. Huo, H. Li, Y. Lu, *J. Am. Chem. Soc.* **2007**, *129*, 8406; b) J. Qi, K. Zhao, G. Li, Y. Gao, H. Zhao, R. Yu, Z. Tang, *Nanoscale* **2014**, *6*, 4072.

[7] a) X.-C. Huang, Y.-Y. Lin, J.-P. Zhang, X.-M. Chen, *Angew. Chem. Int. Ed.* **2006**, *45*, 1557; *Angew. Chem.* **2006**, *118*, 1587; b) K. S. Park, Z. Ni, A. P. Côté, J. Y. Choi, R. Huang, F. J. Uribe-Romo, H. K. Chae, M. O'Keeffe, O. M. Yaghi, *Proc. Natl. Acad. Sci. USA* **2006**, *103*, 10186.

[8] a) K. J. Lee, J. H. Lee, S. Jeoung, H. R. Moon, *Acc. Chem. Res.* **2017**, *50*, 2684; b) Y.-Z. Chen, R. Zhang, L. Jiao, H.-L. Jiang, *Coord. Chem. Rev.* **2018**, *362*, 1; c) Y. V. Kaneti, J. Tang, R. R. Salunkhe, X. Jiang, A. Yu, K. C.-W. Wu, Y. Yamauchi, *Adv. Mater.* **2017**, *29*, 1604898; d) H. B. Wu, X. W. Lou, *Sci. Adv.* **2017**, *3*, eaap9252; e) Z. Liang, C. Qu, D. Xia, R. Zou, Q. Xu, *Angew. Chem. Int. Ed.* **2018**, *57*, 9604; *Angew. Chem.* **2018**, *130*, 9750.

[9] F. Zhang, Y. Wei, X. Wu, H. Jiang, W. Wang, H. Li, *J. Am. Chem. Soc.* **2014**, *136*, 13963.

[10] H.-L. Jiang, B. Liu, Y.-Q. Lan, K. Kuratani, T. Akita, H. Shioyama, F. Zong, Q. Xu, *J. Am. Chem. Soc.* **2011**, *133*, 11854.

[11] a) P. Song, M. Luo, X. Liu, W. Xing, W. Xu, Z. Jiang, L. Gu, *Adv. Funct. Mater.* **2017**, *27*, 1700802; b) Y. Cheng, S. Zhao, B. Johannessen, J.-P. Veder, M. Saunders, M. R. Rowles, M. Cheng, C. Liu, M. F. Chisholm, R. D. Marco, H.-M. Cheng, S.-Z. Yang, S. P. Jiang, *Adv. Mater.* **2018**, *30*, 1706287; c) Z. Li, D. Wang, Y. Wu, Y. Li, *Natl. Sci. Rev.* **2018**, *5*, 673; d) F. Li, G.-F. Han, H.-J. Noh, S.-J. Kim, Y. Lu, H. Y. Jeong, Z. Fu, J.-B. Baek, *Energy Environ. Sci.* **2018**, *11*, 2263; e) F. Yang, P. Song, X. Liu, B. Mei, W. Xing, Z. Jiang, L. Gu, W. Xu, *Angew. Chem. Int. Ed.* **2018**, *57*, 12303; *Angew. Chem.* **2018**, *130*, 12483; f) R. Qin, P. Liu, G. Fu, N. Zheng, *Small Methods* **2018**, *2*, 1700286.

[12] a) Y.-X. Zhou, Y.-Z. Chen, L. Cao, J. Lu, H.-L. Jiang, *Chem. Commun.* **2015**, *51*, 8292; b) S. Chen, J. Bi, Y. Zhao, L. Yang, C. Zhang, Y. Ma, Q. Wu, X. Wang, Z. Hu, *Adv. Mater.* **2012**, *24*, 5593.

[13] a) Q. Lin, X. Bu, A. Kong, C. Mao, X. Zhao, F. Bu, P. Feng, *J. Am. Chem. Soc.* **2015**, *137*, 2235; b) J. Wei, D. Zhou, Z. Sun, Y. Deng, Y. Xia, D. Zhao, *Adv. Funct. Mater.* **2013**, *23*, 2322; c) M. Ding, H.-L. Jiang, *ACS Catal.* **2018**, *8*, 3194; d) L. Liang, C. Liu, F. Jiang, Q. Chen, L. Zhang, H. Xue, H.-L. Jiang, J. Qian, D. Yuan, M. Hong, *Nat. Commun.* **2017**, *8*, 1233.

[14] a) J. Song, Z. Zhang, S. Hu, T. Wu, T. Jiang, B. Han, *Green Chem.* **2009**, *11*, 1031; b) A. C. Kathalikkattil, D.-W. Kim, J. Tharun, H.-G. Soek, R. Roshan, D.-W. Park, *Green Chem.* **2014**, *16*, 1607.

Manuscript received: November 27, 2018
Revised manuscript received: December 10, 2018
Accepted manuscript online: December 19, 2018
Version of record online: January 24, 2019

 © 2019 Wiley-VCH Verlag GmbH & Co. KGaA, Weinheim